INVESTIGATION OF THE BEHAVIOR OF WEAKENED AND STRENGTHENED STEEL COLUMN-BEAM CONNECTIONS UNDER SEISMIC EFFECTS

Ali Koken [1,*] and E. Tuba Hatipoglu [2]

[1] *Assistant Professor, Department of Civil Engineering, Engineering Faculty, Selcuk University, Konya, Turkey*
[2] *Civil Engineer, Konya Provincial Administration, Turkey*
**(Corresponding author: E-mail: akoken@selcuk.edu.tr)*

Received: 14 March 2012; Revised: 4 August 2012; Accepted: 3 January 2013

ABSTRACT: Newly developed solution techniques were used for the beam to column connections of the steel structures after the 1994 Northridge and 1995 Kobe earthquakes. Two significant methods, the use of reduced beam sections and strengthened beam to column connections, are the methods most frequently studied in recent years.
In this study, an experimental procedure was performed to prevent the damages occurring at the beam to column connections of the buildings during an earthquake. For this purpose, four test specimens of beam to column connections were produced. While the first specimen was a strengthened beam to column connection, the second and third were weakened specimens with 40% and 45% ratios, respectively. Additionally, an extra reference specimen (the fourth) was produced to compare the test results. Additionally, a calculation of the analytical force and moment capacities of the test specimens, and the experimental and analytical results were evaluated. The use of reduced beam sections and strengthened beam to column connections favorably affected the behavior of the frame system in a manner that the failure formation occurred not at the connection members but at the end-sections of the beams.

Keywords: Steel frame, steel beam to column connection, seismic behavior of beam to column connections, weakened beam cross-section.

1. INTRODUCTION

Unexpected failures were observed at the beam to column connections of the buildings after the Northridge (1994) and Hyogo-ken Nanbu, Kobe (1995) earthquakes (Hatipoglu [1]).

Rigorous post-earthquake investigations have revealed many factors contributing to the failure. The high stress concentration at the welded web and flanges and the vulnerability of the connection to the large ductility demand are considered to be two critical factors causing such failures (Pachoumis et al. [2], FEMA 350 [3], Engelhardt et al. [4], Tsai et al. [5], Plumier [6]).

A number of improved beam-to-column connection design strategies have been proposed (FEMA 350 [3]), many of which have shown to exhibit satisfactory levels of ductility in numerous tests. Two key concepts have been developed to provide a highly ductile response and reliable performance, and strengthening the connection and/or weakening the beam framing into the connection to avoid damages to the respective column (Pachoumis et al. [7]).

Reduced beam section connections have been shown to exhibit satisfactory levels of ductility in numerous tests and has found broad acceptance (Bruneau et al. [9]; Chen et al. [10]; Plumier [11]; Zekioglu et al. [12]; Engelhardt et al. [13]; Jones et al. [14]; Uang et al. [15]; Lee et al. [16]). In reduced beam section connections, a portion of the beam flanges at a short distance from the column are strategically trimmed to remote stable yielding at the reduced section, and to effectively protect the more vulnerable beam-to-column groove welded joints (Lee et al. [8]).

Some design parameters are recommended by FEMA 350 [3] and FEMA 351 [17] regarding the location and reduction rate of a reduced beam section, based on the local performance of tested beam-to-column assemblies. In Europe, also, following the spirit of the above-mentioned recommendations, in Eurocode 8, Part 3, the designs of such connections are presented. The values for the geometrical parameters recommended in Eurocode 8 are also recommended in FEMA 350 [3], due to the lack of experimental studies on European profiles. Thus, the effectiveness of these recommendations is questionable. Recent experimental research (Pachoumis et al. [2]) confirmed the need for readjustment of the geometrical characteristics for the design of a radius-cut reduced beam section.

Although the concept of weakening the beam to strengthen the steel frame can be thought as meaningless, experimental studies on this subject presented a high level of performance for this type of beam to column connection (Hatipoglu [1]).

In this study, three test specimens were produced and tested under reversed-cyclic loading to prevent the problems experienced at the beam to column connections of the typical forehead-panel beam to column connection. While the first specimen had beam strengthening (N4), the other two had 40% (N2) and 45% (N3) circular weakening in accordance with FEMA 350 [3] and Eurocode 8, respectively. Additionally, a reference specimen (N1) was produced and tested to compare the results. At the end of the tests, the obtained values were evaluated and compared with each other (Hatipoglu [1]).

2. EXPERIMENTAL PROGRAM

2.1 Method

In this study, four beam to column connections with different connection characteristics were produced and tested under reversed-cyclic vertical loads applied at the beam ends. The required loading and displacement data were recorded during the tests using a computer-aided data acquisition system.

2.2 The Material and Cross-section Characteristics

In this study, four different test specimens produced in the laboratory were tested under reversed-cyclic vertical loading applied at the beam-ends. The columns (IPE400 profile) had 400 mm height and 180 mm width, while the column flange and web had the dimensions of 13.5 mm and 8.6 mm, respectively. The beams (IPE270 profile) had a height of 270 mm and a width of 135 mm, with a 10.2 mm beam flange and a 6.6 mm beam web.

The coupon specimens used for the tests, which were obtained by cutting the profiles to determine the mechanical properties of the profiles, were subjected to an axial tensile test. The mechanical properties obtained as a result of the tensile tests are given in Table 1 (Hatipoglu [1]).

Table 1. Mechanical Characteristics of IPE Profiles Used for the Tests

Mechanical Characteristics			
Yield stress	(f_y)	(N/mm²)	302
Ultimate stress	(f_u)	(N/mm²)	448
Young's modulus	(E)	(N/mm²)	203000

2.3 The Characteristics of the Test Specimens

In this study, the aforementioned four specimens having different cross-sections and beam to column connections were tested under reversed-cyclic vertical loading. The first specimen was the reference specimen (N1), whose beam cross-section was not subjected to any weakening or strengthening process. The beam cross-sections of the second and third specimens were weakened circularly in accordance with FEMA 350 [3], Eurocode 8 [18], and the Turkish Earthquake Code [19], in a manner that the top and bottom flanges of the second specimen (N2) were subjected to 40% weakening, while the third (N3) had 45% reduction. Finally, the fourth specimen (N4) was strengthened using a stiffness panel at the beam-end (Hatipoglu [1]). The properties of the test specimens and the beam to column connection photographs are presented in Figure 1.

Test specimens | Beam-to-column connection

Specimen N1

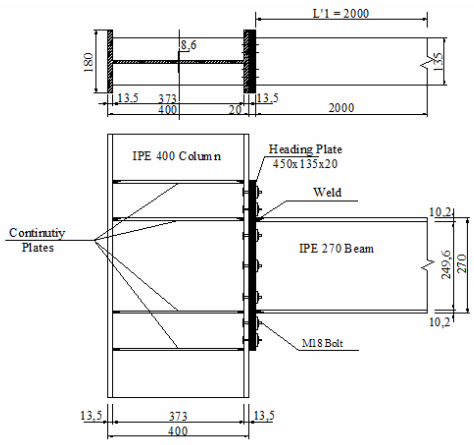

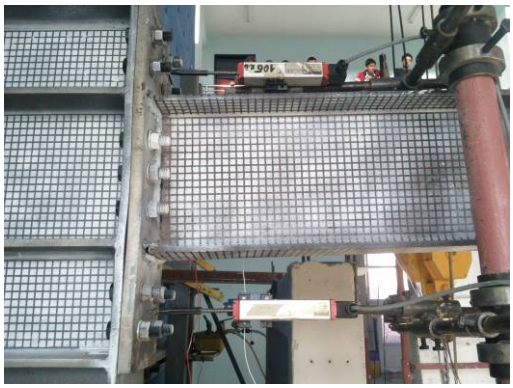

Specimen N2

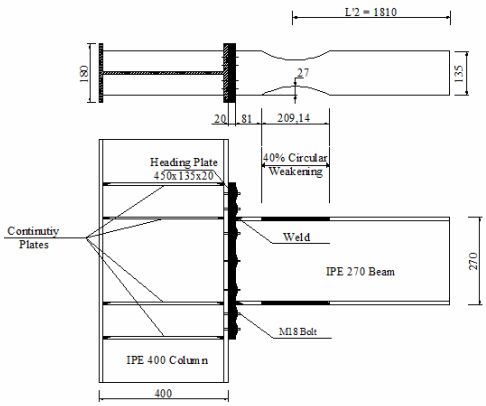

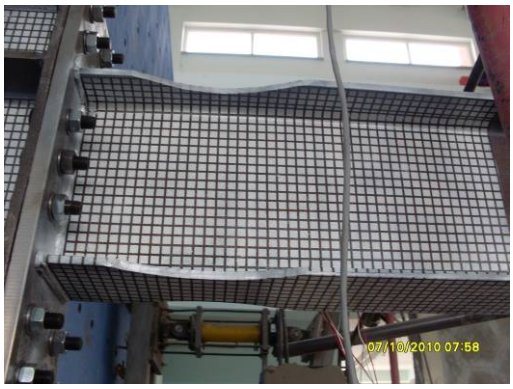

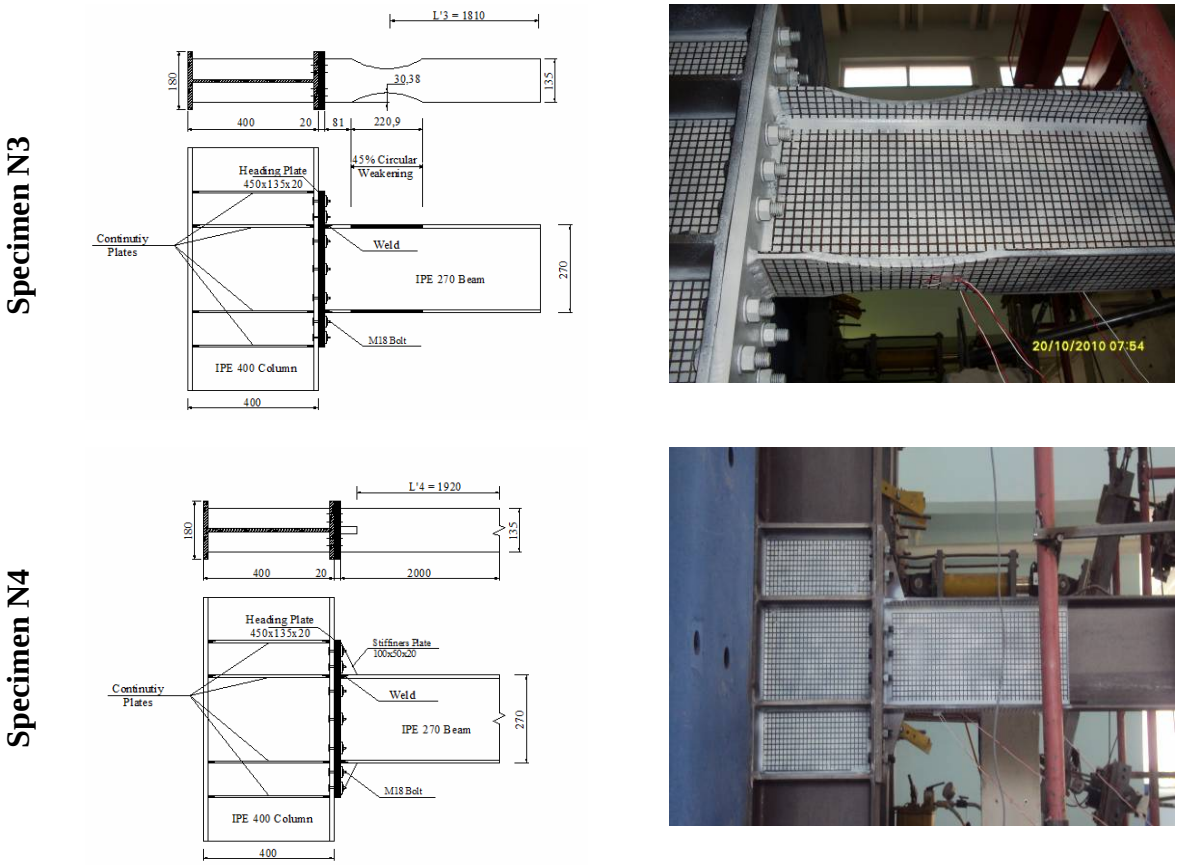

Figure 1. Properties (in mm) of the Test Specimens and Beam to Column Connections

2.4 Experimental Set-up

Four different beam to column connection specimens, which were designed in a manner that they could be loaded from the beam-ends, were tested in this study. Due to the fact that the 3 m column of the specimen was fixed to the rigid wall securely, any rotation or shifting at the supports of the system was prevented. Furthermore, the 2 m beam was connected to the mid-span of the column with a 63×20×3 cm flange plate using filled welding and M18 bolts. During the formation of the connection, maximum welding thickness was applied to prevent failure not at the welding site, but at the beam. Continuity plates and stiffness plates were used at the beam to column connection to strengthen the column panel region. Additionally, a reversed cyclic load was applied at the beam-end using a hydraulic jack and a pump, and recorded by the aid of a load cell. The test mechanism can be seen in Figure 2.

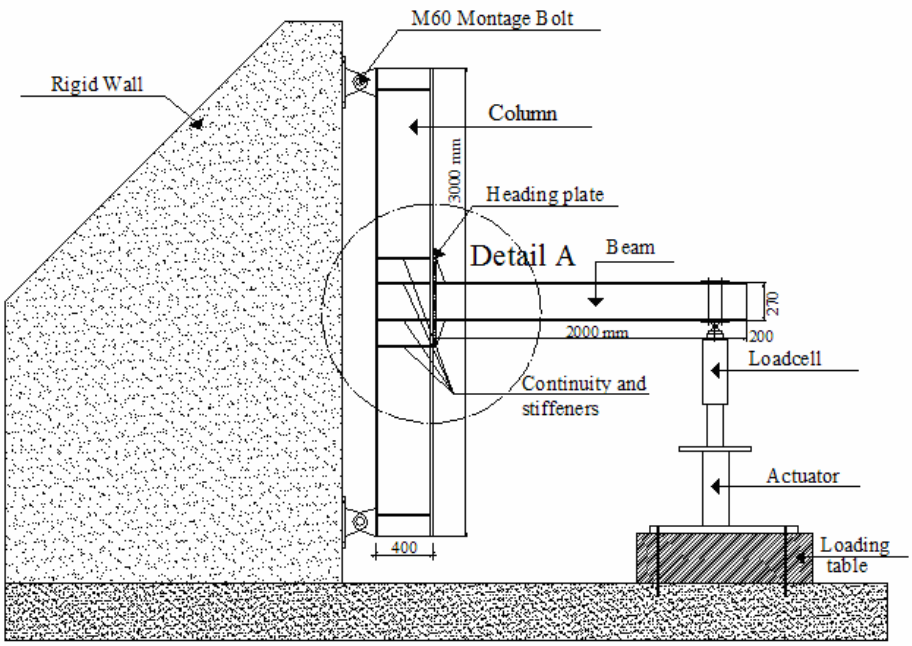

Figure 2. Experimental Set-up

2.5 Measurement Mechanism and Loading Program Used in the Tests

The measuring system of the test mechanism was built taking the test data for each beam to column connection from the same points of the specimens to the greatest extent possible. The displacement measurements were performed with the assistance of four linear variable differential transformers to understand the behavior of the beam to column connection by determining the displacements at the beam-ends and at the mid-points of the columns. Additionally, the measurement of force (F) applied by a hydraulic jack was recorded using a load cell (Figure 3).

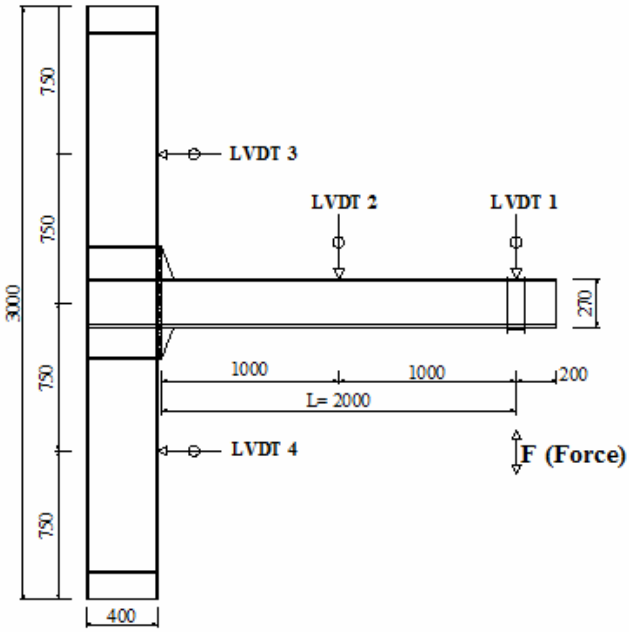

Figure 3. Measurement Mechanism Used in the Tests (in mm)

The loading program used in the tests is given in Table 2 where the rotation (Φ) is calculated dividing the displacement (δ) measured at the beam-end during the test by LVDT-1 to the beam span length (L=2000 mm).

Table 2. Loading Protocol

Load step	Rotation (Φ=δ /L) (Radian)	Number of cycles (nj)	Displacement (δ) (mm)
1	0.00375	2	7.5
2	0.00500	2	10
3	0.00750	2	15
4	0.01000	4	20
5	0.01500	2	30
6	0.02000	2	40
7	0.03000	2	60
8	0.04000	2	80
9	0.05000	2	100
10	0.06000	2	120

3. ANALYSIS ON THE EXPERIMENTAL RESULTS

The experimental results were evaluated in consideration of the properties of the test specimens appropriate to the objective of this study. Therefore, the test specimens were compared to each other in terms of strength envelope, stiffness reduction, and energy consumption capacity (Hatipoglu [1]).

The strength envelopes of the aforementioned specimens are given in Figure 4 where force (F) denotes the force applied at the beam-end using a hydraulic jack and a pump, and recorded by a load cell, and the displacement (δ) indicates the displacement obtained at the beam-end by LVDT-1 shown in Figure 3.

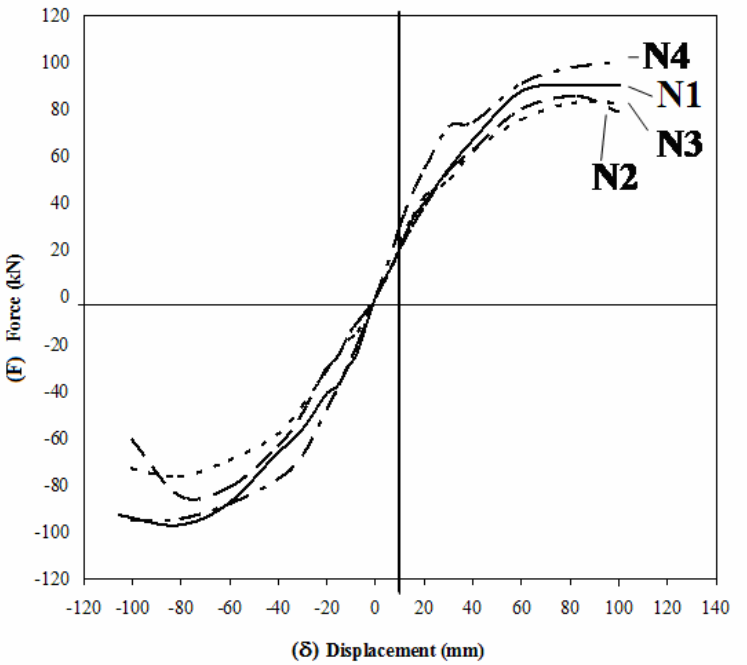

Figure 4. Strength Envelopes of the Test Specimens

As seen in Figure 4, the maximum average horizontal load-bearing values were determined as 96.95 kN (N1), 85.48 kN (N2), 82.83 kN (N3), and 101.60 kN (N4) respectively. When the N1 specimen that was not weakened or strengthened was considered as the reference, the N2 specimen was weakened with 40%, the N3 specimen was weakened with 45%, and the strengthened N4 specimen carried 12% less, 15% less and 5% more load, respectively. The displacement value of 100 mm and the drift ratio (δ/L) of 0.05 corresponding to the maximum loading value were reached for all the test specimens. After the boundary states of yielding and buckling were performed at these levels for the beam cross-section, the failure boundary states for the specimens were reached by the ruptures that occurred at the welding of the connection points.
Stiffness degradation diagrams obtained by the tests of the aforementioned specimens are given in Figure 5, where the stiffness value for each cycle was calculated using the following equation in which the forces (F_1, F_2) and the displacements (δ_1, δ_2) were obtained from the Force-Displacement diagram.

$$Rigidity = \frac{|F_1| + |F_2|}{|\delta_1| + |\delta_2|} \tag{1}$$

The drift ratio was obtained by dividing the displacement (δ) at the beam-end to the span length (L = 2000 m) of the beam.

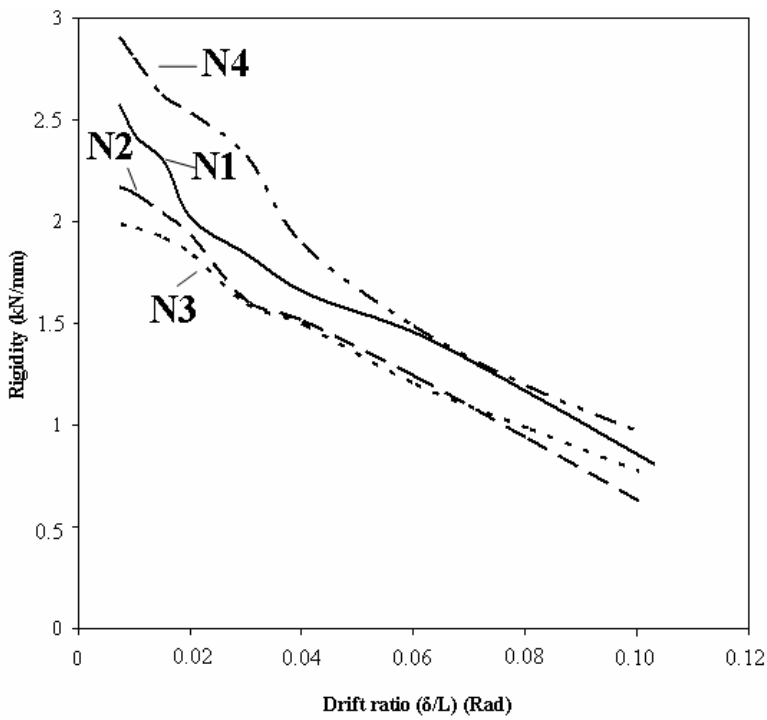

Figure 5. Stiffness Degradation Diagrams of the Test Specimens

As seen in Figure 5, although the first cycle stiffness values were calculated as 2.57 kN/mm (N1), 2.17 kN/mm (N2), 1.99 kN/mm (N3), and 2.91 kN/mm (N4), they decreased in the progressive cycles. The stiffness degradation occurred slightly more rapidly for the N2 and N3 specimens (having weakened cross-sections) in comparison to the other specimens. If the initial stiffness value of specimen N1 was taken as the "reference", the specimens N2, N3, and N4 would have 16% less, 23% less, and 13% more initial stiffness values, respectively. As observed at the end of the tests, the specimens of drift ratio level (δ/L=0.100) had stiffness values below 1 kN/mm. The final stiffness values for this level were obtained as 0.811, 0.630, 0.775, and 0.971 for specimens N1, N2, N3, and N4, respectively.

The energy consumption was determined by calculating the areas inside the hysteretic load-displacement loops for each cycle, disregarding displacements beyond which lateral strength reduction was reached. In Figure 6, the cumulative energy consumption values were plotted against the corresponding cumulative drift ratio Σ(δ/L) that was calculated by successive summation of peak displacement ratios.

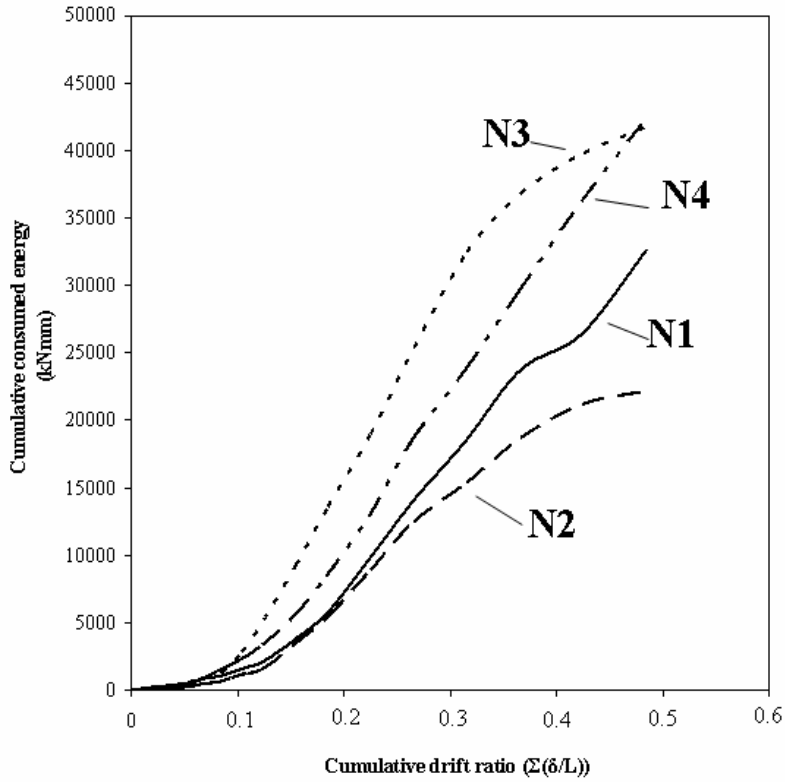

Figure 6. Diagrams of the Energy Consumption Capacities of the Test Specimens

As seen in Figure 6, the cumulative consumed energy values of the test specimens were obtained as 32,590 kNmm, 22,194 kNmm, 41,817 kNmm, and 42,374 kNmm, when the cumulative drift ratio (Σδ/L) was 0.484. When the reference specimen N1 was considered, the specimens N2, N3, and N4 consumed 32% less, 28% more, and 30% more energy, respectively. The cause of less energy consumption for specimen N2 was due to the presence of a welding problem in this specimen earlier than the others (welding rupture).

4. ANALYTICAL STUDY

The test specimens were modeled using actual dimensions and material properties. However, after performing the supporting process of the columns and the application of F (force) at the beam-end according to the test mechanism, the static analysis of the system was executed and the cross-sectional influences were obtained. The force-bearing and moment-carrying capacities for the yielding and plastic boundary states of the test specimens were determined by the aid of the cross-sectional characteristics, material properties, and the cross-sectional influences of the specimens, which were obtained from the static analysis.

The moment bearing capacities can be calculated by using Eqs. 2 and 3 for yielding (elastic) and failure (plastic) states depending on the geometrical and strength characteristics of the beam cross-sections.

$$M_y = f_y \times W_e \quad (2)$$

$$M_p = f_y \times W_p \quad (3)$$

In these expressions;
f_y: The yielding stress (302 N/mm^2) of the material with which the test specimens were produced.
M_y: The maximum moment carried by the beam for yielding (elastic) state.
M_p: The maximum moment carried by the beam for failure (plastic) state.
W_e: The strength moment calculated for elastic state.
W_p: The strength moment calculated for plastic state.

Additionally, the reductions applied at the beam flange cross-sections were taken into account in determining the strength moments.

The force-moment relationship of the beam as a result of the static analysis can be expressed as in Eq. 4;

$$M = F \times L'_i \quad (4)$$

In these expressions;
M: the maximum moment occurred at the beam under the force F,
F: the force acting at the beam-end
L'_i : is the beam span length, i.e. it is the distance between force and the column surface for N1 specimens (L'_1), it is the distance between force and the weakest cross-section at which reduction was made at the beam for N2 (L'_2) and N3 specimens (L'_3), and it is the distance between force and the end-point of the stiffness plate for N4 specimens (L'_4), as given in Figure 1.

Since $M = M_r$ for boundary states, the following expression can be written using the Eqs. 2, 3 and 4.

After substituting Eq. 2 into Eq. 3, load F can be determined using Eq. 4 for the boundary states.

$$F_y = \frac{f_y \times W_e}{L'_i} \quad (5)$$

$$F_p = \frac{f_y \times W_p}{L'_i} \quad (6)$$

- *Analytical calculations for yielding state:* For the yielding state, the yielding stress and the elastic strength moment of the cross-section were used as stated above for the calculation of the yielding force F_y and the yielding moment M_y.

- *Analytical calculations for plastic state:* For the plastic state, the yielding stress and the plastic strength moment of the cross-section were used as stated above for the calculation of the yielding force F_p and the yielding moment M_p. Eq. 7, given similarly both in TEC [19] and FEMA 350 [3], was taken as the base during the plastic moment calculation.

$$M_p = 1.1 \times D_a \times W_p \times f_y \quad (7)$$

The increasing coefficient, D_a, in this expression varies between 1.1–1.2 depending on the material class and member type.

The calculations were carried out for each test specimen according to the principles explained above, and the analytical results were presented in Table 3 together with the experimental results.

Table 3. Analytical and Experimental Force-bearing Capacities of the Test Specimens

SPECIMEN	W_e (cm^3)	W_p (cm^3)	L'_i (mm)	Analytical Calculations				F_p/F_y *(8)/(6)*	Exp. F_{max}	Exp. F_{max}/ *Anal.* F_p *(10)/(8*
				M_y (kNm)	F_y (kN)	M_p (kNm)	F_p (kN)			
(1)	*(2)*	*(3)*	*(4)*	*(5)*	*(6)*	*(7)*	*(8)*	*(9)*	*(10)*	*(11)*
N1	429	484	2000	130	64.78	193	96.47	1.49	96.95	1.00
N2	282	330	1810	85	46.94	132	72.59	1.55	85.48	1.18
N3	264	311	1810	80	44.00	124	68.59	1.56	82.83	1.21
N4	429	484	1920	130	67.51	193	100.54	1.49	101.60	1.01

5. RESULTS

The following results were obtained from the experimental and analytical studies.

1. As a result of the tests, the maximum shear force carried by the beam was 101.60 kN for specimen N4, and thus, specimen N4 carried 5% more shear force (moment), in comparison to the reference specimen, N1. The specimens N2 and N3 carried 12% and 15% less shear force, respectively, than that of the reference specimen N1 (Table 4).

2. When the initial stiffness values were considered, the maximum stiffness value was 2.57 kN/mm for specimen N4. Specimens N4, N2, and N3 had 13% more, 16% less, and 23% less initial stiffness values, respectively, in comparison to the stiffness value of specimen N1 (Table 4).

3. When the consumed energy values were considered, specimen N4 had the maximum consumed energy of 42,374 kNmm. Specimens N4, N3, and N2 consumed 30% more, 28% more, and 32% less energy, respectively, when compared to that of the reference specimen N1. Specimen N2's lower energy consumption was due to the welding problem N2 faced earlier than the other specimens (Table 4).

Table 4. Results Obtained from the Experimental Studies

Experimental Results				
Specimen	F_{max} *(kN)*	Max. Stiffness *(kN/mm)*	Stiffness degradation (Final stiffness/Initial stiffness)	Cumulative consumed energy *(kN×mm)*
N1	96.95	2.57	0.811 / 2.57 = 0.32	32590
N2	85.48	2.17	0.630 / 2.17 = 0.29	22194
N3	82.83	1.99	0.775 / 1.99 = 0.39	41817
N4	101.60	2.91	0.971 / 2.91 = 0.33	42374

4. When comparing the experimental and analytical results:

- The maximum shear force values obtained and calculated for specimens N1 and N4 were almost the same. Moreover, the experimental shear force values obtained for specimens N2 and N3 (having reduced cross-sections) were 20% more than the values obtained by the analytical solution.
- During the analytical calculations, the "Da" coefficient was taken as 1.2, and the actual cross-sectional characteristics were used for the reduced cross-sections. The formula proposed for plastic calculations presented much closer results to the exact values for the other specimens, but a lower amount of deviation was observed for the reduced cross-sections. Therefore, a reevaluation of the formula used for the analytical calculations of the reduced cross-sections can be considered.

5. When the failure types of the test specimens were considered, yielding occurred at the top and bottom flanges of the steel beam during the further cycle stages at maximum stress levels. Buckling occurred at the flanges and moved through the beam body in the subsequent stages. At this time, the damage formation at the welding was observed. In particular, the rupturing of the flange weldings during the test on specimen N2 was experienced earlier than expected. This state did not have a significant effect on maximum shear force and moment values, but caused less stiffness and energy consumption than expected.

6. CONCLUSIONS

The following conclusions were obtained in light of the experimental and analytical studies.

- The strengthening of the beam cross-section at the beam to column connection using a stiffness panel increased the beam shear force and also the moment capacity.
- The use of a stiffness panel at the beam to column connection increased the initial stiffness, and the reduction at the beam-cross section decreased the initial stiffness by 20%.
- As a general expression, both strengthening the cross-section using a stiffness panel and making a reduction at the beam cross-section increased the consumed energy by nearly by 30%, which favorably affects the performance of this type of system under seismic conditions.
- According to the results obtained by the analytical solution, the bearing shear force values of the test specimens for failure boundary states (plastic states) were 49-55% larger than those for the yielding boundary states for all the specimens.

The use of reduced beam sections and strengthened beam to column connections favorably affected the behavior of the frame system in a manner that the failure formation occurred not at the connection members, but at the end-sections of the beams. Additionally, the use of a strengthened beam to column connection considerably increased the force and moment carrying capacities, initial stiffness, and energy consumption capacities of the steel frames. Therefore, the use of reduced beam sections and strengthened beam to column connections can be suggested for the steel frame constructions under the risk of earthquake forces.

ACKNOWLEDGEMENT

This study was supported by Scientific Research Projects Office of Selcuk University in the scope of Project No: 10201032. The experimental data used for the study was provided from the Master of Science dissertation titled "Weakened and Strengthened Type Steel Column-Beam Junctions to Investigate the Behavior under Earthquake Loading" (Hatipoglu [1]).

REFERENCES

[1] Hatipoglu, E.T., "Weakened and Strengthened Type Steel Column-Beam Junctions To Investigate The Behavior Under Earthquake Loading", Master of Science Dissertation, Selcuk University, Institute of Graduate and Applied Sciences, Konya, Turkey, 2011.

[2] Pachoumis, D.T, Galoussis, E.G., Kalfas, C.N. and Efthimiou, I.Z.,"Cyclic Performance of Steel Moment-resisting Connections with Reduced Beam Sections-experimental Analysis and Finite Element Model Simulation", Engineering Structures, 2010, Vol. 32, pp. 2683-2692.

[3] FEMA 350, "Recommended Seismic Design Criteria for New Steel Moment-frame Buildings", Washington (DC), 2000.

[4] Engelhardt, M.D. and Husain, A.S., "Cyclic-loading Performance of Welded Flange-bolted Web Connections", J. Struct. Eng., 1993, Vol. 119, No. 12, pp. 3537-3549.

[5] Tsai, K.C., Shun, W. and Popov, E., "Experimental Performance of Seismic Steel Beam to Column Moment Joints", J. Struct. Eng., 1995, Vol. 121, No. 6, pp. 925-931.

[6] Plumier, A., "Behaviour of Connections", J. Constr. Steel Res., 1994, Vol. 29, pp.95-119.

[7] Pachoumis, D.T., Galoussis, E.G., Kalfas, C.N. and Efthimiou, I.Z., "Reduced Beam Section Moment Connections Subjected to Cyclic Loading: Experimental Analysis and FEM Simulation" Engineering Structures, 2009, Vol. 31, pp.216-223.

[8] Lee, C.H. and Chung, S.W., "A Simplified Analytical Story Drift Evaluation of Steel Moment Frames with Radius-cut Reduced Beam Section", Journal of Constructional Steel Research, 2007, Vol. 63, pp. 564–570.

[9] Bruneau, M, Uang, C.M. and Whittaker A., "Ductile Design of Steel Structures", New York: McGraw-Hill; 1998.

[10] Chen, S.J., Yeh, C.H. and Chu, J.M., "Ductile Steel Beam-to-column Connections for Seismic Resistance", Journal of Structural Engineering ASCE, 1996, Vol. 122, No. 11, pp. 1292–1299.

[11] Plumier, A., "The Dogbone: Back to the Future", Engineering Journal AISC, 1997, Vol. 34, No. 2, pp.61–67.

[12] Zekioglu, A., Mozaffarian, H., Chang, K.L. and Uang, C.M., "Designing after Northridge", Modern Steel Construction AISC, 1997, Vol. 37, No. 3, pp. 36–42.

[13] Engelhardt, M.D., Winneberger, T., Zekany, A.J. and Potyraj, T.J., "Experimental Investigations of Dogbone Moment Connections", Engineering Journal AISC, 1998, Vol. 35, No. 4, pp. 128–139.

[14] Jones, S.L, Fry, G.T. and Engelhardt, M.D., "Experimental Evaluation of Cyclically Loaded Reduced Beam Section Moment Connections", Journal of Structural Engineering ASCE, 2002, Vol. 128, No. 4, pp. 441–451.

[15] Uang, C.M. and Fan, C.C., "Cyclic Stability Criteria for Steel Moment Connections with Reduced Beam Section", Journal of Structural Engineering ASCE, 2001, Vol. 127, No. 9, pp. 1021–1027.

[16] Lee, C.H, Jeon, S.W., Kim, J.H. and Uang, C.M., “Effects of Panel Zone Strength and Beam Web Connection Method on Seismic Performance of Reduced Beam Section Steel Moment Connections”, Journal of Structural Engineering ASCE, 2005, Vol. 131, No. 12, pp. 1854–1865.

[17] FEMA 351, “Recommended Seismic Evaluation and Upgrade Criteria for Existing Welded Steel Moment Frame Buildings”, Washington (DC), 2000.

[18] EC 8. “Part 3: Design of Structures for Earthquake Resistance, Assessment and Retrofitting of Buildings”, EN 1998-3, June 2005.

[19] Turkish Earthquake Code (TEC), Ankara, Turkey, 2007.